

Received 20 March 2023, accepted 2 April 2023, date of publication 11 April 2023, date of current version 19 April 2023.

Digital Object Identifier 10.1109/ACCESS.2023.3266330

RESEARCH ARTICLE

Model Predictive Control for Energy-Efficient Yaw-Stabilizing Torque Vectoring in Electric Vehicles With Four In-Wheel Motors

SANG HYUK KIM^{1,2} AND KWANG-KI K. KIM^{1,3}

¹Department of Electrical and Computer Engineering, Inha University, Incheon 22212, Republic of Korea

²Department of Electrical Engineering, Inha University, Incheon 22212, Republic of Korea

³Research and Development Division, Hyundai Motor Company, Hwaseong-si, Gyeonggi-do 18280, Republic of Korea

Corresponding author: Kwang-Ki K. Kim (kwangki.kim@inha.ac.kr)


This work was supported by the Basic Science Research Program through the National Research Foundation of Korea (NRF) funded by the Ministry of Education under Grant NRF-2019M3F2A1073401.

ABSTRACT This paper considers the problem of stabilizing and energy-efficient torque vectoring for electric vehicles with four independent in-wheel motors. In electric vehicles with four in-wheel motors, four electric motors are separately attached to the four wheels without an extra drive shaft. The mechanical and structural nature enables reduction of energy loss during power transmission and securing extra interior space. In addition, independent control of wheel torques can provide better yaw motion stability and improved energy efficiency. This paper proposes two model predictive control (MPC) methods for stability-constrained energy-efficient torque vectoring of four in-wheel motor electric vehicles. For the adaptive weighting factors of multiple objective functions of reference tracking and energy saving, we use exponential functions that vary with the lateral motion and steering input. Depending on the optimal control problem formulation with different dynamical system equations and constraints, the associated predictive controller can be represented as either a linear parameter-varying MPC (LPV-MPC) or nonlinear MPC (NMPC). For LPV-MPC, longitudinal and lateral motions are decoupled, whereas the coupled dynamics of the two-track model are exploited in NMPC. For comparisons and demonstrations of LPV-MPC and NMPC in the MPC of torque vectoring, three driving scenarios are simulated with a high-fidelity vehicle simulation solution, CarMaker (IPG Automotive). In comparison with the built-in IPG driver implemented in CarMaker, we demonstrate fuel efficiency improvements of over 2–3 % on average with guaranteed yaw stability.

INDEX TERMS Four in-wheel motor electric vehicles, torque vectoring, fuel efficiency, EV range extension, yaw stability, optimal control, linear parameter-varying model predictive control, nonlinear model predictive control.

I. INTRODUCTION

In accordance with the increased environmental concerns and enhanced governmental regulations worldwide, many automobile original equipment manufacturer have spurred the development of electric vehicles (EVs) and are gradually reducing the production of engine vehicles [2]. Energy efficiency and range extension are important factors in the development and widespread adoption of EVs. Various methods for extending the EV maximum driving range have

The associate editor coordinating the review of this manuscript and approving it for publication was Jie Gao .

been proposed from both hardware and software perspectives. One of which is to adopt in-wheel motor vehicles, in which the wheels are mechanically combined with electric machines. Development of four in-wheel-motor electric vehicles (4IWMEVs) has been considered as a useful strategy for the current electric vehicle trend that places importance on the utilization of interior space and energy efficiency [3].

Recently, in the automobile industry, torque vectoring (TV) systems have been used to improve driving stability and energy efficiency [4]. TV systems generate the vehicle's yaw moment directly through torque distribution among the four wheels, on which the four independent electric machines

are mounted [5]. Various TV methods have been applied to improve the driving stability and energy efficiency of 4IWMEVs [6], [7]. In 4IWMEVs, four independent forces generated from the wheels produce a combined torque such that the resulting control system is over-actuated. Many techniques have been studied in both industry and academia to determine the optimal torque distribution by vectorizing forces or torques.

The TV control system of 4IWMEVs can be used to improve the robustness, energy efficiency, and driving stability of electric vehicles. In particular, various optimal control techniques are used to improve fuel efficiency by minimizing fuel or energy consumption while imposing constraints on the actuation limits and vehicle stability. In [8], a classical linear quadratic regulator (LQR) feedback controller method was used to improve the energy efficiency of battery electric vehicles (BEVs). In [9], an LQR-based low-level TV controller was combined with a high-level TV controller based on nonlinear model predictive control (NMPC) to achieve the driving stability and energy efficiency improvement of 4IWMEVs. In [9], a fuzzy logic-based weight-tuning method was integrated into a multi-objective NMPC framework, and a real-time implementation using the rapid control prototyping equipment, dSPACE MicroAutoBoxII, was also presented. The authors of [10] proposed an integrated controller based on NMPC, in which torque vectoring and vertical movement were considered for energy efficiency improvement.

In [11], a yaw moment controller was designed based on a Lyapunov stability condition. The authors of [12] verified the energy efficiency improvement in the cornering state through direct yaw moment control of 4IWMEVs. In [13], a fuzzy control method was proposed for corner-driving of 4IWMEVs to guarantee driving stability and derive energy efficiency improvement by switching among the three cornering modes. The authors of [14] proposed a method for determining the yaw rate reference model using a lookup table to improve the energy efficiency in the direct yaw moment control of 4IWMEVs. Fuzzy and PID control methods are difficult to improve energy-efficiency from an optimal control perspective. Recently, MPC and LQR-based torque vectoring system controllers have been proposed and it is important for tuning optimal controllers adapted to the driving conditions and situations of the vehicle.

In [15], optimal torque vectoring for two yaw-rate controllers was applied to four wheel drive (4WD) formal type vehicles. One is H_∞ -based optimal control and the other is an linear parameter varying (LPV) controller. The author of [16] presents a torque vectoring control strategy for rear-wheel steering vehicles using NMPC for which the Pontryagin's minimum principle (PMP) is used to reduce NMPC's computational burden and validate controller performance in real time in hardware-in-the-loop (HIL) environment.

In this paper, we propose intelligent torque vectoring predictive controllers that optimize energy-efficiency and vehicle stability by the adaptation of the optimal control

parameters to driving conditions. The primary contributions of this paper can be summarized as follows:

- Different from [1], we consider the objective function that is dependent of the driver's steering angle. In addition, for better evaluation of control performances, MPC-based controller is executed within a high-fidelity vehicle simulator, IPG CarMaker.
- We propose two predictive control methods using linear and nonlinear models for stabilizing and energy-efficient TV of 4IWMEVs. While existing work [15], [16] considers predictive control with a linear or nonlinear model, our work investigates performances of predictive controllers with LPV and nonlinear models that reflect the change of vehicle speed as an endogenous variable. In the case of predictive control using a linear model, the existing lateral dynamics model and the longitudinal dynamics model are combined to consider vehicle speed as an additional state variable. In addition, the controller is designed with a linear parameter varying-model predictive control (LPV-MPC) using a speed-dependent LPV model. For energy efficiency, the total mechanical energy of the motors is considered so that the resulting optimal control problem can be represented as a quadratic program (QP). For the NMPC formulation, the total electric energy consumed by the four motors is considered as an objective function and modeled using appropriate polynomial regressors.
- The cost function of the proposed optimal control problems is designed to minimize the multiple objectives considering driving stability and energy consumption. The weights for the multiple objective functions are adaptively determined by considering the vehicle motion and the steering requirement. To deliver the motion required by the driver's steering commands, the tires are steered to change the vehicle's heading angle accordingly. Aggressive cornering requires higher weight in yaw stability whereas energy efficiency is a dominant factor for straight driving. To reflect tradeoffs between different requirements, the weights are set as exponential functions of the steering angle.
- We validate and verify the performances of the proposed LPV-MPC and NMPC methods for the TV of 4IWMEVs with comparisons to the existing IPG Driver available in a vehicle simulator, CarMaker. The degree of improvement in driving stability and energy efficiency is compared and analyzed by applying the TV controller designed with the LPV-MPC and NMPC to the actual driving cycle. Four model predictive controllers are designed for the case where the weight of the objective function changes and the case where it does not change according to the driving situation of the vehicle and various driving cycles. For the four designed TV controllers, the performances of the driving stability and energy efficiency improvement according to each driving scenario are investigated with comparisons of each other and the built-in IPG Driver in CarMaker.

This paper is organized as follows: Section II discusses the modeling and yaw stability of in-wheel motors and presents the background required for energy-efficient TV controller design. Section III discusses the system model, reference input model, and objective function constraints for applying the model predictive control method. An objective function in continuous time is then introduced to improve the driving stability and energy efficiency of the 4IWMEVs through the TV controller. Section IV defines the optimal control problem by applying the LPV-MPC and NMPC to the TV controller. Subsequently, a method of determining the weighting parameters for optimal control is discussed. Section V analyzes the results of vehicle simulation using a TV controller designed with LPV-MPC and NMPC and compares the performance of the controller.

II. BACKGROUND

A. IN-WHEEL MOTOR MODELING

An in-wheel motor is a combination of an electric machine and an inverter and is directly mounted inside the wheel. The driving method of a vehicle equipped with an in-wheel motor is more advanced than that for all-wheel driving. Currently, 4IWMEVs are not yet commercially available, but research is being conducted to improve driving stability, energy efficiency, and commercialization potential by making 4IWMEVs in-house at research facilities [17], [18].

In this study, modeling of powertrain was carried out using a permanent magnet synchronous motor (PMSM)-based in-wheel motor. PMSMs have the advantages of good energy efficiency in power conversion, low heat generation, optimal control within the maximum torque range of the motor, and smooth and fast response to continuous changes. However, it also has disadvantages such as high cost, a complicated motor setup, and complexity in control. EVs equipped with in-wheel motors can independently apply wheel-torques, which enables the quick responses in acceleration, deceleration, and turning motion control. In addition, driving stability and energy efficiency can be improved by applying an appropriate TV system.

The longitudinal dynamics representing the relationship between the longitudinal force and torque of the in-wheel motor is considered as:

$$J_m \dot{\omega}_{ij} = T_{ij} - F_{ij} R_{eff} \quad (1)$$

where ω_{ij} is the wheel angular speed, R_{eff} is the effective radius of the tire and J_m is the combined rotational inertia of the wheel and motor. The variables T_{ij} and F_{ij} ($i \in \{\text{front}, \text{rear}\}$, $j \in \{\text{left}, \text{right}\}$) are the torques and longitudinal forces applied to the four wheels, respectively. One of the characteristics of in-wheel motor vehicles is that torque can be independently applied to each of the four wheels. Therefore, there are four inputs to control the three state variables, which can take advantage of the over-actuated system.

At the time of this research, some companies such as Protein Electric [19] and Elaphe [20] are developing in-wheel

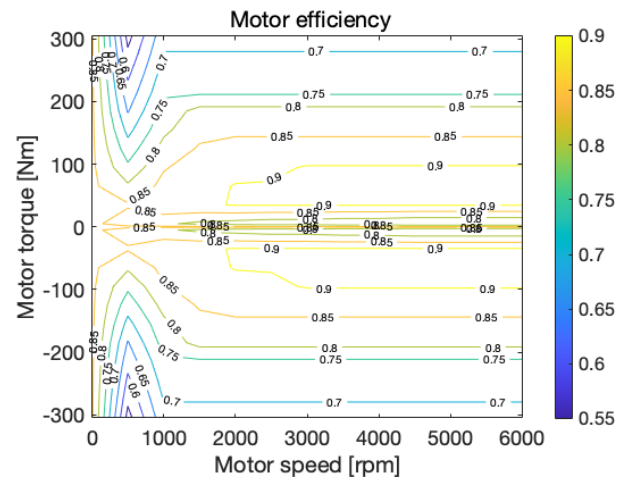


FIGURE 1. Motor efficiency map (PRIUS-JPN30) generated from the data available in CarSim [21].

motors and specific hardware specifications are being proposed. In this study, the existing commercial electric motor, PRIUS-JPN30, is considered as an in-wheel motor and its CarSim data is used for modeling in optimal control and closed-loop simulations. Fig. 1 shows the efficiency map for PRIUS-JPN30. The continuous quasi-static motor model of power-conversion efficiency and constant torque and power limits are used for optimal control problem formulations to reflect realistic applications. In addition, the numerical data associated with Fig. 1 are also used for building a polynomial-based regression model of the electric motor power in terms of the wheel torques and rotation speed. In Section III-E, the torque and angular velocity data of motor experiments are used for training the model by least-squares methods.

B. FACTORS FOR CONSIDERING DRIVING STABILITY

The most important factor in a vehicle's cornering is stability. When the driver applies the steering angle, the yaw of the vehicle and the speed yaw required by the driver are generated according to the vehicle model [22]. To consider the yaw stability, the difference between the yaw rate requested by the driver and the actual yaw rate of the vehicle are considered. In this study, the driving stability improvement was derived by utilizing the advantages of the in-wheel motor. In minimizing the objective function, the difference between the actual rate of the vehicle and the rate requested by the driver is considered as the objective function.

In the single-track model, as shown in Fig. 2, consider the understeering gradient K_v as in (2).

$$K_v = \frac{l_r m}{C_{\alpha,f}(l_f + l_r)} - \frac{l_f m}{C_{\alpha,r}(l_f + l_r)} \quad (2)$$

where m is the vehicle mass, $C_{\alpha,f}$ and $C_{\alpha,r}$ are the front and rear cornering stiffnesses of the vehicle, respectively, and l_f and l_r are the distance from the vehicle's center of gravity to the front and rear axles, respectively. The cornering stiffness

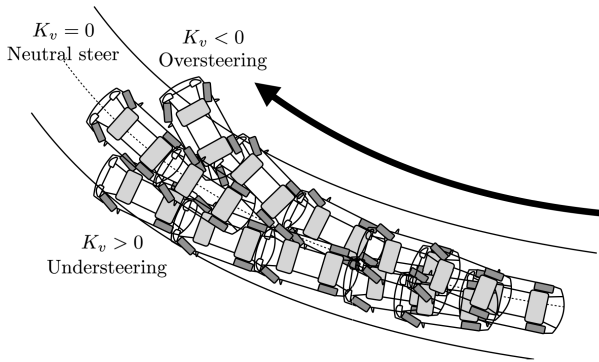


FIGURE 2. Lateral motion schematic for oversteering ($K_v < 0$), understeering ($K_v > 0$) and neutral steering ($K_v = 0$) for corner-driving.

is a variable representing the relationship between the tire slip angle α_i and the lateral force $F_{y,i}$ of the tire:

$$F_{y,i} = C_{\alpha,i} \alpha_i \quad (3)$$

where the tire slip angles are approximated as

$$\alpha_f \approx \beta - \delta + \frac{l_f \psi}{v} \text{ and } \alpha_r \approx \beta - \frac{l_r \psi}{v}. \quad (4)$$

where v is the vehicle speed, δ is the steering angle, and ψ is the yaw angle of the vehicle-body. The cornering stiffness $C_{\alpha,i}$ tends to remain constant when the slip angle is smaller than 5° . If the side slip angle becomes excessively large, the tire loses linearity in (3) and the driver may not be able to drive in the required direction with respect to the required steering angle [23]. Therefore, the body side slip angle β should remain in certain bounds, as discussed in Section III-D.

III. OPTIMAL CONTROL FORMULATION

When the IPG driver applies the required speed v_{des} through the steering angle δ and APS or BPS input according to the driving situation in Fig. 3, the reference input is calculated from the reference model block accordingly. The steering angle δ is applied as the wheel steering angle through the electrical power steering (EPS) system after considering the maximum and minimum steering angles of the wheels with respect to the steering angle applied by the IPG driver [24]. When the calculated reference input is applied to the MPC controller, the optimal input required for motor torque is derived through LPV-MPC or NMPC in consideration of the constraints. This is transmitted to each of the four motors of the vehicle, and the resulting actual motor torque $T_{actual,ij}$ is generated, directly producing a yaw moment, and TV is applied. Using $T_{actual,ij}$ and ω_{ij} , the energy usage is calculated from the powertrain and the battery SoC is calculated based on it. The lateral accelerations a_y , $\dot{\psi}$, and v can be used as measurement data while the vehicle is driving. Based on this, through the state estimator, the yaw rate $\dot{\psi}$, side slip angle β , and vehicle speed v of the next state are determined by the LPV-MPC or NMPC-applied controller. It is applied as an initial value for the prediction.

A. REFERENCE MODEL

The driver's requested state variable $\dot{\psi}_{des}$ by the driver's requested steering angle δ , speed v , and K_v of (2) can be derived as follows [9]:

$$\dot{\psi}_{des} = \frac{v/l}{1 + K_v v^2} \delta \quad (5)$$

where $l = l_f + l_r$ is the length of the vehicle-body. To prevent oversteering and understeering, we consider the reference input of the yaw-rate defined as

$$\dot{\psi}_{ref} = \min \{ |\dot{\psi}_{des}|, |\dot{\psi}_{max}| \} \cdot \text{sgn}(\delta) \quad (6)$$

where $\dot{\psi}_{max}$ is the allowable maximum yaw-rate that is defined later in (25) and $\text{sign}(\delta)$ is the sign of the current steering angle δ . In addition, the reference side slip angle β_{ref} is considered from the viewpoint of the driving stability of Section II-B and is typically set to zero [25], [26].

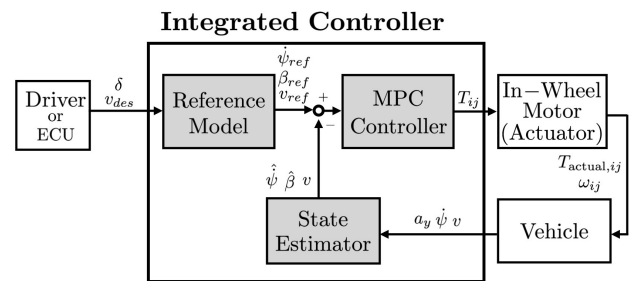


FIGURE 3. Schematic diagram of an integrated TV controller of 4IWM/EVs.

The reference input for vehicle speed v_{ref} is determined by the maximum/minimum values $a_{x,max}$ and $a_{x,min}$ of the vehicle's longitudinal acceleration using v_{des} , the maximum values of the lateral acceleration $a_{y,max}$, and the curve κ of the driving course as follows. If the radius of curvature of the driving course is R , then κ is obtained as

$$\kappa = \frac{1}{R} = \frac{\dot{\psi}_{des}}{v_{des}}. \quad (7)$$

Using the above data, v_{ref} is obtained through the built-in function in IPG CarMaker as follows:

$$v_{ref} = h(v_{des}, a_{x,max}, a_{x,min}, a_{y,max}, \kappa). \quad (8)$$

where the closed-form of the function h is not explicitly given here due to an intellectual property issue.

B. LONGITUDINAL VEHICLE DYNAMICS MODEL

For LPV model of vehicle dynamics, the lateral dynamics model and the longitudinal dynamics model can be combined. We consider the following longitudinal vehicle dynamics:

$$m\dot{v} = F_{xf} + F_{xr} - F_{aero} - R_{xf} - R_{xr} - mg \sin \theta \quad (9)$$

where F_{xf} and F_{xr} are the longitudinal forces of the front and rear tires, respectively, and R_{xf} and R_{xr} are the forward

and rearward forces, respectively, that depend on road grades. Additionally, F_{aero} can be considered as follows:

$$F_{aero} = c_{aero} A_L \frac{\rho}{2} (v + v_{wind})^2 \quad (10)$$

where c_{aero} , A_L , and ρ are the aerodynamic drag coefficient, front area, and air density, respectively. In this study, the load forces induced by the inclination angle of the road grade θ and wind speed v_{wind} were not considered. They can be incorporated as measurable or estimated external disturbances in predictive models, which implies that the methods of MPC proposed in this paper can be straightforwardly extended to consider the road grade θ and wind speed v_{wind} as well. Expressing F_{xf} and F_{xr} with the power of the four wheels is as follows:

$$m\dot{v} = \sum_{i \in \{f,r\}, j \in \{r,l\}} F_{ij} - c_{aero} A_L \frac{\rho}{2} v^2 \quad (11)$$

For linearization of (11) the truncated first-order Taylor series is used:

$$m\dot{v} = \sum_{i \in \{f,r\}, j \in \{r,l\}} F_{ij} - (\rho c_{aero} A_L \bar{v})v + \frac{(\rho c_{aero} A_L \bar{v}^2)}{2} \quad (12)$$

that scan be rewritten as a state space model

$$\dot{v} = A_{lon}v + B_{long}u \quad (13)$$

where the system parameters are given as

$$A_{lon} = -\frac{\rho c_{aero} A_L \bar{v}}{m}, \quad B_{long} = \frac{1}{mr_w} [1 \ 1 \ 1 \ 1], \quad (14)$$

and $u = [T_{fl} \ T_{fr} \ T_{rl} \ T_{rr}]^T$ is the control input vector.

C. LATERAL VEHICLE DYNAMICS MODEL

In this paper, the lateral motion of the vehicle was modeled considering the following assumptions:

- The cornering stiffness $C_{\alpha,ij}$ for each of the four wheels had a constant value for each side slip angle.
- The rear wheel steering angle, δ_r , was set to 0. That is, it is only steered by the front wheels.
- The left and right steering angles of the front wheels are the same: $\delta = \delta_{fl} = \delta_{fr}$.
- Roll and pitch motion are not taken into account.

1) DOUBLE TRACK MODEL

In Fig 4, the lateral motion equation considering the change in vehicle speed, yaw rate, and side slip angle is as follows [27]:

$$\begin{aligned} \dot{v} = & \frac{1}{m} \left\{ (F_{fl} + F_{fr}) \cos(\delta - \beta) \right. \\ & + (F_{rl} + F_{rr} - c_{aero} A_L \frac{\rho}{2} v^2) \cos \beta \\ & - (C_{\alpha,fl} + C_{\alpha,fr}) \left(\delta - \beta - \frac{l_f \dot{\psi}}{v} \right) \sin(\delta - \beta) \\ & \left. + (C_{\alpha,fl} + C_{\alpha,fr}) \left(-\beta + \frac{l_r \dot{\psi}}{v} \right) \sin \beta \right\} \quad (15) \end{aligned}$$

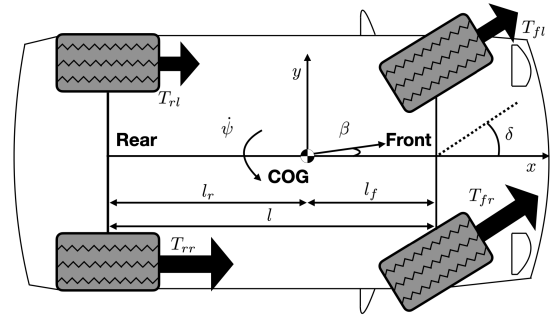


FIGURE 4. Double track model used as a nonlinear predictive model for NMPC.

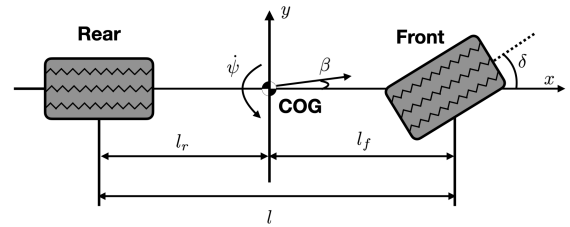


FIGURE 5. Single track model used as a linear predictive model for LPV-MPC.

$$\begin{aligned} \ddot{\psi} = & \frac{1}{J_z} \left\{ l_f (F_{fl} + F_{fr}) \sin \delta \right. \\ & + l_f (C_{\alpha,fl} + C_{\alpha,fr}) \left(\delta - \beta - \frac{l_f \dot{\psi}}{v} \right) \cos \delta \\ & + \frac{b_f}{2} (F_{fr} - F_{fl}) \cos \delta \\ & - \frac{b_f}{2} (C_{\alpha,fr} - C_{\alpha,fl}) \left(\delta - \beta - \frac{l_f \dot{\psi}}{v} \right) \sin \delta \\ & - l_r (C_{\alpha,rl} + C_{\alpha,rr}) \left(\beta + \frac{l_r \dot{\psi}}{v} \right) \\ & \left. + \frac{b_r}{2} (F_{rr} - F_{rl}) \right\} \quad (16) \end{aligned}$$

$$\begin{aligned} \dot{\beta} = & \frac{1}{mv} \left\{ (C_{\alpha,fl} + C_{\alpha,fr}) \left(\delta - \beta - \frac{l_f \dot{\psi}}{v} \right) \cos(\delta - \beta) \right. \\ & + (F_{fl} + F_{fr}) \sin(\delta - \beta) \\ & - (F_{rl} + F_{rr} - c_{aero} A_L \frac{\rho}{2} v^2) \sin \beta \\ & \left. + (C_{\alpha,rl} + C_{\alpha,rr}) \left(-\beta + \frac{l_r \dot{\psi}}{v} \right) \cos \beta \right\} - \dot{\psi}, \quad (17) \end{aligned}$$

where J_z is the amount of energy that the vehicle tries to maintain when cornering. The double-track model is used as a predictive model when designing a TV controller to which an NMPC is applied.

2) SINGLE TRACK MODEL

To make (15), (16), and (17) into state space matrices, it is necessary to introduce a single-track model, shown in Fig. 5. This single-track model is valid when compared to the real

model when the lateral acceleration is less than $0.4g [m/s^2]$. Therefore, it is less accurate than the double-track model, but it has the advantage of being an easy to design linear model predictive controller. For the single-track model, the cornering stiffness of the two wheels is considered as follows:

$$C_{\alpha,f} = \frac{C_{\alpha,fl} + C_{\alpha,fr}}{2} \text{ and } C_{\alpha,r} = \frac{C_{\alpha,rl} + C_{\alpha,rr}}{2}. \quad (18)$$

To satisfy the validity of the single-track model, the lateral dynamics model is simplified based on the following small angle assumptions: $\sin \delta \approx 0$, $\cos \delta \approx 1$, $\sin \beta \approx 0$, $\cos \beta \approx 1$. By adding the linearized dynamics (12), representing the force in the longitudinal direction, to the single-track state space model above, the system state equations can be expressed as

$$\dot{\mathbf{x}}_{lat} = A_{lat}(v)\mathbf{x}_{lat} + B_{lat}\mathbf{u} + D_{lat}(v)\delta \quad (19)$$

where the matrices are defined as

$$A_{lat}(v) = \begin{bmatrix} \frac{l_f^2 C_{\alpha,f} + l_r^2 C_{\alpha,r}}{mv^2} & -\frac{l_f C_{\alpha,f} - l_r C_{\alpha,r}}{mv} \\ \frac{J_z v}{mv^2} & \frac{J_z}{mv} \\ \frac{l_{\alpha,r} C_{\alpha,r} - l_f C_{\alpha,f}}{mv^2} & -\frac{C_{\alpha,f} + C_{\alpha,r}}{mv} \end{bmatrix}, \quad (20)$$

$$B_{lat} = \begin{bmatrix} \frac{b}{2J_z r_w} & \frac{b}{2J_z r_w} & -\frac{b}{2J_z r_w} & \frac{b}{2J_z r_w} \\ 0 & 0 & 0 & 0 \end{bmatrix}, \quad (21)$$

$$D_{lat}(v) = \begin{bmatrix} \frac{l_f C_{\alpha,f}}{mv} \\ \frac{J_z}{mv} \\ \frac{C_{\alpha,f}}{mv} \end{bmatrix}, \quad (22)$$

and $\mathbf{x}_{lat} = [\dot{\psi} \ \beta]^T$ is the reduced state vector of the lateral motion. By combining the above lateral dynamics with the state-space model in (13), the overall state-space model can be represented as follows:

$$\dot{\mathbf{x}} = A(v)\mathbf{x} + B\mathbf{u} + D(v)\delta + E \quad (23)$$

where $\mathbf{x} = [\dot{\psi} \ \beta \ v]^T$ is the extended state vector, $\mathbf{u} = [T_{fl} \ T_{fr} \ T_{rl} \ T_{rr}]^T$ is the control input vector, and the system parameters are defined as

$$A(v) = \begin{bmatrix} A_{lat}(v) & 0 \\ 0 & A_{lon} \end{bmatrix}, \quad B = \begin{bmatrix} B_{lat} \\ B_{long} \end{bmatrix},$$

$$D(v) = \begin{bmatrix} D_{lat}(v) \\ 0 \end{bmatrix}, \quad E = \begin{bmatrix} 0 \\ 0 \\ \frac{1}{2m}(\rho c_{aero} A_L \bar{v}^2) \end{bmatrix}. \quad (24)$$

The above state space model is an LPV model that changes depending on the vehicle speed v and is used as a predictive model for LPV-MPC.

D. CONSTRAINTS FOR STABILITY GUARANTEE

When the driver demands a high yaw rate from the vehicle, if the road friction coefficient cannot withstand the force of the tire, driving may become unstable owing to understeering or oversteering; therefore, the lateral acceleration of

the vehicle must be limited by the friction coefficient of the road, and the maximum allowable yaw rate is given as the following [22]:

$$\dot{\psi}_{max}(v) = \frac{\mu g}{v} \quad (25)$$

where μ is the road friction coefficient and g is the gravitational acceleration. $\mu \in [0, 1]$ changes depending on the road condition. Typically, μ has a value of $0.1 \sim 0.3$ on snowy roads, $0.5 \sim 0.7$ on wet roads, and $0.8 \sim 1.0$ on normal asphalt roads [28]. Therefore, the maximum allowable side slip angle is limited by considering μ as follows:

$$\beta_{max} = \arctan(0.02\mu g) \quad (26)$$

which is an experimentally obtained equation that ranges from 4° to 10° depending on the road friction coefficient μ .

E. ELECTRIC ENERGY CONSUMPTION MODELING

In this study, energy optimization is considered by minimizing the mechanical or electrical energy consumed (+ sign) and regenerated (- sign) the four electric machines mounted on the wheels.

a: MECHANICAL POWER OF THE MOTOR

When applying the linear model predictive control method, it should be composed of a quadratic form of the objective function. It is difficult to express the electric energy of a motor in a quadratic form. Therefore, in this study, when applying the LPV-MPC, an objective function is set that considers the energy consumption by utilizing the mechanical energy of the motor. The mechanical power of the motor is obtained as follows:

$$P_{mech} = \sum_{i \in \{f,r\}, j \in \{r,l\}} T_{ij} \omega_{ij}. \quad (27)$$

In consideration of the numerical stability, a strictly convex function can be utilized instead:

$$P_{mech} = \sum_{i \in \{f,r\}, j \in \{r,l\}} \gamma T_{ij}^2 + T_{ij} \omega_{ij} \quad (28)$$

where the coefficient $\gamma > 0$ of the quadratic term is set to a small positive number. This makes the cost function P_{mech} strongly positive definite with respect to the torque-vector $\mathbf{u} = [T_{fl} \ T_{fr} \ T_{rl} \ T_{rr}]^T$. The mechanical power of the motor P_{mech} to which the quadratic term is added is a general quadratic form for motor torque, and it is convenient to apply QP. This implies that considering the quadratic terms allows the Hessian of the cost function with respect to control inputs to be strictly positive in the process of numerical optimization so that numerical stability of underlying numerical linear algebra in QP or SQP can be improved.

b: ELECTRICAL POWER OF THE MOTOR

The electric power of the motor is obtained as follows:

$$P_{elec} = \begin{cases} \sum_{i \in \{f,r\}, j \in \{r,l\}} \frac{T_{ij} \omega_{ij}}{\eta_{ij}} & (\text{for } T_{ij} > 0) \\ \sum_{i \in \{f,r\}, j \in \{r,l\}} T_{ij} \omega_{ij} \eta_{ij} & (\text{for } T_{ij} < 0) \end{cases} \quad (29)$$

which is the electric energy calculation of the motor for the driving mode ($T_{ij} > 0$) and the regenerative braking mode ($T_{ij} < 0$). The factor $\eta_{ij} \in (0, 1)$ is the efficiency of the motor of each wheel. When the motors independently mounted on the four wheels are physically the same and the electrical power is $P_{elec,ij}$, a regression model is used to approximate $P_{elec,ij}$ as follows:

$$P_{elec,ij} \approx c_1 \omega_{ij} + c_2 \omega_{ij} T_{ij} + c_3 \omega_{ij} T_{ij}^2 + c_4 \omega_{ij}^2 T_{ij}^2 + c_5 \omega_{ij}^3 T_{ij}^2 \quad (30)$$

where there are five regressors ω_{ij} , $\omega_{ij} T_{ij}$, $\omega_{ij} T_{ij}^2$, $\omega_{ij}^2 T_{ij}^2$, and $\omega_{ij}^3 T_{ij}^2$, and the corresponding c_i coefficients are determined as a least-squares solution.

The approximated $P_{elec,ij}$ in (30) is the result of estimating $P_{elec,ij}$ as a polynomial function composed of the torque and angular velocity of the motor using the efficiency information on the torque and angular velocity of the motor from the efficiency map of the motor. The root mean square error (RMSE) between the calculated actual $P_{elec,ij}$ and the estimated $P_{elec,ij}$ was 344.375 [W], which was set as the basis of the torque and angular velocity of the motor with the smallest RMSE value. The relative RMSE was calculated as 0.3672. Because NMPC solves the optimal control problem using nonlinear programming (NLP), it is suitable to consider the higher-order polynomial form of (30) as the objective function.

In this study, energy is considered as the objective function to consider the energy optimization of a TV system as follows:

$$E_{motor}(t) = \int_0^t P_{motor}(\tau) d\tau \quad (31)$$

where P_{motor} can be either the mechanical or electrical power of the motor. When LPV-MPC is applied, P_{mech} is considered whereas P_{elec} is considered for NMPC.

F. COST FUNCTIONS

In this study, as objective functions in the optimal control algorithm corresponding to predictive control, both the tracking problem considering driving stability and the motor energy consumption considering energy efficiency are considered. The two objective functions to be minimized are defined as follows:

- Reference tracking error of a quadratic form

$$J_1 = \int_0^{t_f} (\mathbf{x}_{ref} - \mathbf{x})^T \mathbf{Q} (\mathbf{x}_{ref} - \mathbf{x}) dt \quad (32)$$

TABLE 1. Motor specifications (PRIUS-JPN30).

Parameter	Value	Unit
Weight	56.75	[kg]
Rotational Inertia [J _m]	0.0226	[kgm ²]
Peak Output Power	30	[kW]
Peak Output Torque [T _{max}]	305	[Nm]
Maximum Speed	6000	[rpm]

where the weighting matrix is set to be diagonal:

$$W = \begin{bmatrix} w_1 & 0 & 0 \\ 0 & w_2 & 0 \\ 0 & 0 & w_3 \end{bmatrix}. \quad (33)$$

- Energy consumption over the traveling time

$$J_2 = E_{motor}(t_f). \quad (34)$$

The energy consumption of the motor E_{motor} is considered as in (31), and the cost function in continuous time can be considered by using J_1 and J_2 , as follows:

$$\begin{aligned} & \text{minimize} && J = \lambda J_1 + (1 - \lambda) J_2 \\ & \text{subject to} && \mathbf{x}(0) = \mathbf{x}_0 \\ & && \frac{d\mathbf{x}}{dt} = F(\mathbf{x}(t), \mathbf{u}(t), \delta(t)) \\ & && T_{\min} \mathbf{1} \leq \mathbf{u}(t) \leq T_{\max} \mathbf{1} \\ & && \dot{\psi}_{\min} \leq \dot{\psi}(t) \leq \dot{\psi}_{\max} \\ & && \beta_{\min} \leq \beta(t) \leq \beta_{\max} \\ & && v_{\min} \leq v(t) \leq v_{\max} \end{aligned} \quad (35)$$

where $\mathbf{1} = [1 \ 1 \ 1 \ 1]^T$ is the all-ones vector and the vector field $F(\mathbf{x}(t), \mathbf{u}(t), \delta(t))$ corresponds to the dynamical system used for a prediction model that is either LPV or nonlinear dynamical system equations. When applying LPV-MPC, (23) is used, and when applying NMPC, (15), (16), and (17) are used. The torque constraint conditions of the motor T_{min} and T_{max} are determined using TABLE 1 as the specifications of the motor and are considered as $T_{min} = -T_{max}$. Similarly, the yaw-rate bounds and the side slip-angle bounds are considered as $\dot{\psi}_{min} = -\dot{\psi}_{max}$ and $\beta_{min} = -\beta_{max}$. The speed limits v_{min} and v_{max} can be considered differently depending on the driving situation, and in this study, it is determined by the speed set by the IPG driver. The cost function J consists of weighted objective functions, the reference tracking error function J_1 and energy-consumption function J_2 . In this study, using the objective function in (35), it is approximately transformed to apply MPC. Section IV deals with the method of determining the objective function of the MPC and the weight of the objective function as the control algorithm of the energy-efficient TV system that guarantees driving stability.

IV. MPC FOR TORQUE VECTORING SYSTEM

A. LPV-MPC METHOD

To control the TV system of four in-wheel motor electric vehicles, the controller is presumed to be designed based

on the nonlinear model owing to the nonlinearity of the lateral vehicle dynamics, and the optimal solution of predictive control should be derived through the NLP method in an optimization view point. However, it may be difficult to implement in real time because of its high computational complexity. In this study, as an alternative to this, we propose an LPV-MPC method that uses a linear predictive model to achieve a performance similar to that of a nonlinear model. Many nonlinear models can be expressed as LPV models, and because LPV models maintain linear properties, a relatively fast computation can be expected [29]. In this study, considering an LPV model, the change in vehicle speed v is considered and reflected in the predictive model. Therefore, in predicting the state and input, the vehicle speed v in that state is reflected in the prediction model at every step. To apply the model predictive control method, a time discretization model assuming a zero-order holder (ZoH) control input is used as follows:

$$A_d(v) = \exp(A(v)\Delta t), B_d(v) = A^{-1}(v)(A_d(v) - I)B,$$

$$D_d = A^{-1}(v)(A_d(v) - I)D(v), E_d(v) = A^{-1}(v)(A_d(v) - I)E$$

where $\exp(A(v)\Delta t) = \sum_{\ell=0}^{\infty} (A(v)\Delta t)^\ell / \ell!$ denotes an exponential matrix. In LPV-MPC, the following time-discretized system model is used for prediction:

$$\begin{aligned} \mathbf{x}(k) &= f_{d,lpv}(\mathbf{x}(k), \mathbf{u}(k), \delta(k)), \\ &= A_d(v)\mathbf{x}(k) + B_d(v)\mathbf{u}(k) + D_d(v)\delta(k) + E_d(v) \end{aligned} \quad (36)$$

where $\delta(k)$ is the steering angle that is controlled by the driver and can be treated as a known or measurable disturbance in predictive control.

For optimality control of the LPV-MPC, the following two objective functions are considered:

$$J_{1,lpv} = \sum_{k=1}^{N_p} (\mathbf{x}(k) - \mathbf{x}_{ref}(k))^T W (\mathbf{x}(k) - \mathbf{x}_{ref}(k)) \quad (37)$$

and

$$J_{2,lpv} = \sum_{k=0}^{N_p-1} \frac{P_{mech}(k) + P_{mech}(k+1)}{2} \Delta t \quad (38)$$

where N_p is the prediction horizon. For implementation of LPV-MPC, it is assumed that the vehicle speed is not varying over the prediction horizon. The mechanical power of the motor P_{mech} in (38) is determined by (28). Using the cost functions given in (37) and (38), the optimal control problem for applying LPV-MPC can be defined as follows:

$$\begin{aligned} &\text{minimize} \quad J_{lpv} = \lambda J_{1,lpv} + (1 - \lambda) J_{2,lpv} \\ &\text{subject to} \quad \mathbf{x}(0) = \mathbf{x}_0 \\ &\quad \mathbf{x}(k+1) = f_{d,lpv}(\mathbf{x}(k), \mathbf{u}(k), \delta(k)) \\ &\quad T_{\min} \mathbf{1} \leq \mathbf{u}(k) \leq T_{\max} \mathbf{1} \\ &\quad \dot{\psi}_{\min} \leq \dot{\psi}(k) \leq \dot{\psi}_{\max} \\ &\quad \beta_{\min} \leq \beta(k) \leq \beta_{\max} \\ &\quad v_{\min} \leq v(k) \leq v_{\max} \end{aligned} \quad (39)$$

where $\mathbf{u}(\cdot)$ is a set of solutions obtained by applying the model prediction control method within the prediction interval N_p . Considering the LPV model, the optimal input that minimizes (39) within the prediction interval and the resulting state variables can be predicted as follows:

$$U_p(k) = \begin{bmatrix} \mathbf{u}_v(k|k) \\ \mathbf{u}_v(k+1|k) \\ \vdots \\ \mathbf{u}_v(k+N_p-1|k) \end{bmatrix}, X_p(k) = \begin{bmatrix} \mathbf{x}_v(k+1|k) \\ \mathbf{x}_v(k+2|k) \\ \vdots \\ \mathbf{x}_v(k+N_p|k) \end{bmatrix} \quad (40)$$

where $\mathbf{u}_v(\cdot)$ and $\mathbf{x}_v(\cdot)$ are the inputs obtained as a solution by applying the prediction technique using the model considering the change in v in (36) and the predicted state variables based on it. In this study, to compare and verify the performance of the model predictive controller designed with the LPV model, the performance of the controller designed with the LPV-MPC method and the controller designed with the NMPC method are compared in terms of computation time and optimality.

B. NMPC METHOD

Because the lateral dynamics linear model of a vehicle is a model established with a small lateral acceleration, it may become inaccurate depending on the curve situation of the vehicle. However, the nonlinear model has a high accuracy in reflecting the actual dynamics of the vehicle; therefore, more accurate results can be obtained by designing a controller based on the nonlinear model. When applying the NMPC, using the dynamical system equations (15), (16), and (17), the nonlinear system model in continuous time can be represented as

$$\dot{\mathbf{x}}(t) = f(\mathbf{x}(t), \mathbf{u}(t), \delta(t)) \quad (41)$$

where $\mathbf{x} = [\dot{\psi} \ \beta \ v]^T$ and $\mathbf{u} = [T_{fl} \ T_{fr} \ T_{rl} \ T_{rr}]^T$. Here, δ is the steering angle of the vehicle that is assumed to be known over the prediction horizon. To consider this as a predictive model of NMPC, when the discretized model using the Euler forward approximation of the equations (15), (16), and (17) is computed, it is considered as a predictive model for applying NMPC:

$$\mathbf{x}(k+1) = f_{d,nmpc}(\mathbf{x}(k), \mathbf{u}(k), \delta(k)). \quad (42)$$

The objective function is set considering driving stability and energy consumption, as in (39):

$$J_{1,nmpc} = \sum_{k=1}^{N_p} (\mathbf{x}(k) - \mathbf{x}_{ref}(k))^T W (\mathbf{x}(k) - \mathbf{x}_{ref}(k)), \quad (43)$$

$$J_{2,nmpc} = \sum_{k=0}^{N_p-1} \frac{P_{elec}(k) + P_{elec}(k+1)}{2} \Delta t \quad (44)$$

where (44) is a non-quadratic function composed of polynomials that are linearly regressed with the torque and angular velocity of the motor, as in (30). Therefore, it is necessary to

solve this problem using the NLP method. In this study, the NLP problem was defined as follows:

$$\begin{aligned}
 &\text{minimize} && J_{\text{nmpc}} = \lambda J_{1,\text{nmpc}} + (1 - \lambda) J_{2,\text{nmpc}} \\
 &\text{subject to} && \mathbf{x}(0) = \mathbf{x}_0 \\
 &&& \mathbf{x}(k + 1) = f_{d,\text{nmpc}}(\mathbf{x}(k), \mathbf{u}(k), \delta(k)) \\
 &&& T_{\min} \mathbf{1} \leq \mathbf{u}(k) \leq T_{\max} \mathbf{1} \\
 &&& \dot{\psi}_{\min} \leq \dot{\psi}(k) \leq \dot{\psi}_{\max} \\
 &&& \beta_{\min} \leq \beta(k) \leq \beta_{\max} \\
 &&& v_{\min} \leq v(k) \leq v_{\max}.
 \end{aligned} \tag{45}$$

C. DEPENDENCE OF COST WEIGHT ON VEHICLE MOTION

In this study, the control of the TV system has two objectives: driving stability and energy efficiency improvement. The weight matrix W in (37) and (43) is a 3×3 diagonal matrix with the weights $w_1, w_2,$ and $w_3,$ and the weight of the motor energy consumption costs in (38) and (44) is defined as the fourth factor $w_4.$ These values should change according to the different driving conditions of vehicle maneuvering. For example, if the vehicle is cornering, driving stability may be more important than improving energy efficiency as opposed to driving straight ahead. Therefore, it is important to determine proper weights of the cost functions of the model-based predictive optimal control.

For adaptively changing the weights in multiple objectives of optimal control, the exponential function of the steering angle is used to depend on the driving situation of the vehicle in determining the weights. The weight factors w_1 and w_2 consider yaw rate tracking and side slip angle tracking and are increased when driving stability is considered, and w_3 and w_4 consider the required speed tracking and energy efficiency. w_3 and w_4 are increased when maintaining a constant speed on a straight road and improve the energy efficiency. The weights $w_1, w_2, w_3,$ and w_4 are considered as the following functions:

$$w_1 = K_1 e^{|\delta|}, \quad w_2 = K_2 e^{|\delta|}, \quad w_3 = K_3 e^{-|\delta|}, \quad w_4 = K_4 e^{-|\delta|}. \tag{46}$$

Notice that the weights in (46) are set to be determined according to the steering angle δ in real time. When the steering angle is increased using the characteristics of the exponential function, w_1 and w_2 increase accordingly. This is to ensure driving stability by assigning weight to the objective function that considers the difference between the yaw rate and side slip angle. Conversely, when the steering angle is closing to 0° (straight driving), the weights w_3 and w_4 increase. This is because when the steering angle is close to $0^\circ,$ the values of the yaw rate and side slip angle are equal or close to zero, so that higher weight is given to the speed tracking and energy efficiency improvement requested by the driver. The weights are selected as exponential functions of the steering angle. The nonlinear characteristics of such weight adaptation to driving conditions help to improve driving stability in cornering and energy efficiency in straight-driving. The parameters $K_1, K_2, K_3,$ and K_4 are appropriate constants that are pre-computed via numerical experiments.

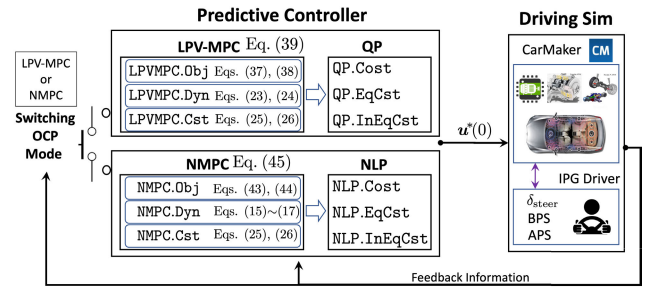


FIGURE 6. A schematic flowchart diagram for two predictive control methods with simulation-based implementations.



FIGURE 7. Simulation of TV control system for 4IWMEVs in a virtual environment using IPG CarMaker. Simulation videos for the driving scenarios in Sections V-A, V-B, and V-C can be found at: <https://www.youtube.com/playlist?list=>

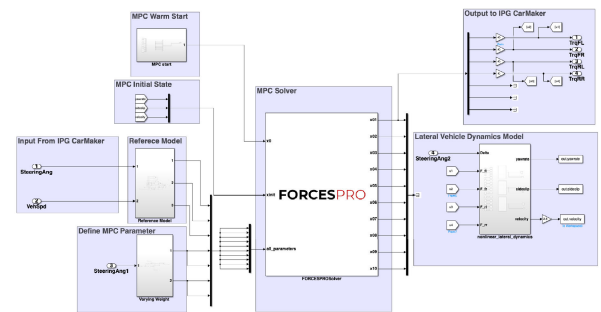


FIGURE 8. Simulink model for the closed-loop control system simulations of predictive control-based torque vectoring.

V. SIMULATION RESULTS

In the previous section, we presented two methods of predictive control for optimal torque vectoring. Fig. 6 shows a flowchart of two predictive control methods, LPV-MPC and NMPC, for torque vectoring and a simulation-based implementation. For real vehicle implementations, Driving Sim will be replaced by an actual in-wheel motor EV and a human driver.

Four controllers were designed using LPV-MPC and NMPC, and the performances of the four controllers were verified through simulation with IPG CarMaker and MATLAB/Simulink in Fig 7. The details of Simulink model for closed-loop simulations are presented in Fig. 8. The four types of designed controllers are as follows:

- VW LPV that applies the LPV-MPC where the weights of the multiple objective functions change according to the vehicle motion and steering command.
- NVW LPV that applies the LPV-MPC where the weights of the multiple objective functions are set as constants.
- VW NMPCA that applies the NMPC where the weights of the multiple objective functions change according to the vehicle motion and steering command.
- NVW NMPC that applies the NMPC where the weights of the multiple objective functions are set as constants.

The RMSE for reference input, energy consumption, and computation time were used as performance comparison indicators to compare the performance of the above controller. For the LPV-MPC method, the problem was solved by using the FORCESPRO QP solver with a dense QP formulation and an interior-point method (IPM), and simulation with IPG CarMaker was performed using the S-function of Simulink. FORCESPRO makes the design of embedded predictive controllers simple and the computation time is fast and accurate [30], [31].

The NMPC method solves the NLP problem using the nonlinear primal-dual interior point method (PD-IPM) of the solver, FORCESNLP, available at FORCESPRO. Note that all predictive controllers (linear, nonlinear, and LTV) are computed by the PD-IPM with warm-start, which could reduce a lot of the online computation time. The driving scenario consisted of three scenarios, and the driving track Nurbuergring Grandprix Course and FS Germany 2015 were considered to compare the energy consumption of the actual vehicle with the slalom lane change.

The IPG CarMaker’s Demo car was selected as the vehicle model. When simulating four predictive controllers in IPG CarMaker, all vehicle parameters including motor specifications are set to be the same. In addition, the driver’s steering angle and required speed in each scenario are set to be the same. For all four model prediction control methods, the prediction horizon N_p was set to 10, and the step size Δt was set to 0.02 sec. This implies that the optimal control input in MPC was calculated by predicting the future of 0.2 sec driving. In addition, it was assumed that the road friction coefficient μ is 0.9 for a general asphalt road in all three scenarios. To verify the performance of the TV controller in which the model predictive control method is applied, the results of improved driving stability and energy efficiency are demonstrated by applying the TV system by comparing it with the driving results of the IPG driver in CarMaker. It is assumed that the state can be estimated from measurements and we use the data obtained through the side slip angle sensor model available in IPG CarMaker.

A. SLALOM CHANGE SIMULATION

Scenario 1 considers the slalom lane-change situation. The steering angle and speed were applied according to the situation using the IPG driver model. The total distance was set at 600 m. When the steering angle and speed are determined by the IPG driver, the yaw rate reference input is

TABLE 2. <Scenario 1> Comparison of RMSE according to yaw rate reference input when driving with TV controller designed with four different predictive control methods and utilizing IPG driver.

Control method	Reference input tracking RMSE
NVW LPV	0.1042
VW LPV	0.1042
NVW NMPC	0.1033
VW NMPC	0.1035
IPG Driver	0.1037

TABLE 3. <Scenario 1> Comparison of RMSE according to each reference input of side slip angle ($\beta_{ref} = 0$) when driving with the TV controller designed with four predictive control methods and driving of the IPG driver.

Control method	Reference input tracking RMSE
NVW LPV	0.0398
VW LPV	0.0398
NVW NMPC	0.0405
VW NMPC	0.0398
IPG Driver	0.0394

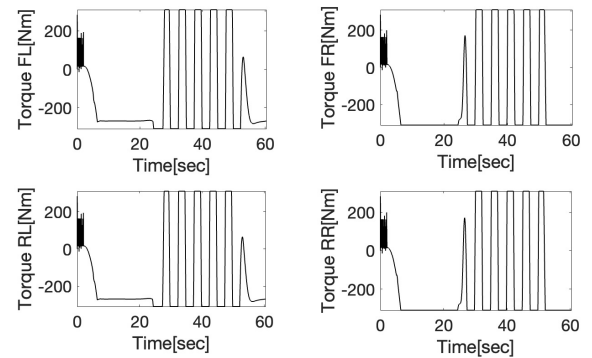


FIGURE 9. <Scenario 1> Motor demand torque applied to four in-wheel motors as a result of TV with NVW LPV-MPC applied.

determined accordingly, and the tracking problem is constructed by considering this in the objective function. To compare the performance of the controller, the RMSE between the reference input and the actual yaw rate of the vehicle is compared in TABLE 2. The smallest RMSE value occurred when NVW NMPC was applied, and the largest RMSE occurred when LPV MPC was applied, regardless of weight change. This is because the model accuracy was not guaranteed owing to the frequent steering angle application. As shown in Scenarios 1 and 3, the frequent steering angle application shows a smaller RMSE value when the nonlinear model is used as a predictive model. The RMSE considering the difference from the actual data for the reference input of the side slip angle is shown in TABLE 3. The controller designed by the NVW NMPC showed the highest RMSE value and the lowest RMSE value was shown when driving with the IPG CarMaker’s built-in controller (IPG Driver).

As one can observe the demanded torques of four different controllers in Figs. 9~12, a phenomenon occurred in that the solution of the predictive control method designed with a

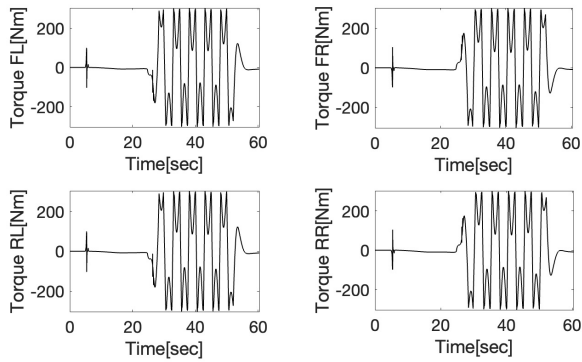


FIGURE 10. <Scenario 1> Motor demand torque applied to four in-wheel motors as a result of TV with VW LPV-MPC applied.

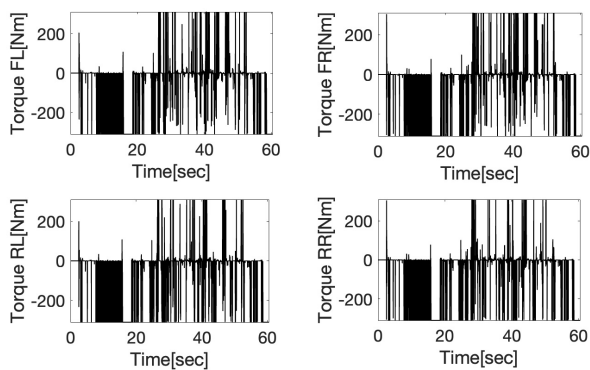


FIGURE 11. <Scenario 1> Motor demand torque applied to four in-wheel motors as a result of TV with NVW NMPC applied.

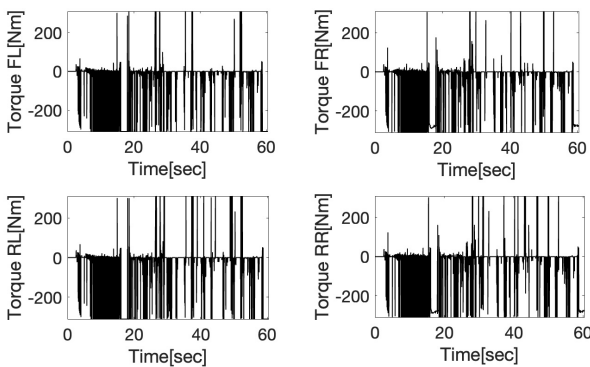


FIGURE 12. <Scenario 1> Motor demand torque applied to four in-wheel motors as a result of TV with VW NMPC applied.

nonlinear model resulted in a relatively conservative solution compared with the solution of the LPV-model based predictive control method. In addition, whenever the driver applies a large steering angle value, the maximum torque is applied to the wheels on both sides of the vehicle and the maximum yaw moment is generated. This shows the same tendency in Scenarios 2 and 3 in Figs. 16~19, 23~26. In TABLE 4, the lowest energy consumption was observed when VW LPV-MPC was applied among the five results. In addition,

TABLE 4. <Scenario 1> Comparison of energy consumption of four wheel motors when driving with the TV controller designed with four predictive control methods using motor power data of IPG CarMaker and driving with the IPG driver.

Control method	Motor energy consumption [Wh]
NVW LPV	144.8891
VW LPV	144.7648
NVW NMPC	144.8437
VW NMPC	144.8497
IPG Driver	147.8451

TABLE 5. <Scenario 1> Comparison of fuel efficiency when driving with the TV controller designed with four predictive control methods and driving with the IPG driver.

Method	Fuel efficiency [km/kWh]	Relative fuel efficiency [%]	Final SoC [-]
NVW LPV	4.1463	102.05	0.6976
VW LPV	4.1490	102.11	0.6975
NVW NMPC	4.1469	102.06	0.6975
VW NMPC	4.1476	102.08	0.6975
IPG Driver	4.0634	100	0.6975

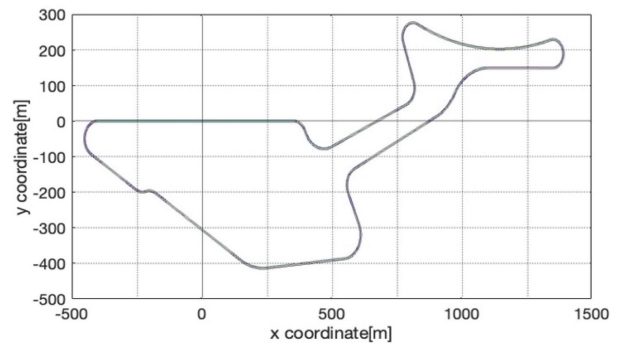


FIGURE 13. <Scenario 2> Nurbuergring Grandprix course.

both VW LPV and VW NMPC show lower energy consumption than NVW LPV and NVW NMPC because of the weight of the objective function considering the driving situation.

By using the motor energy data from the results of applying each control method, the fuel efficiency was calculated based on the assumption that there is no energy used in the air conditioning system or lamp. The results of calculating the average fuel efficiency when driving to the final destination are shown in TABLE 5. In TABLE 6, the fuel efficiency is improved by approximately 2.11 % in the VW LPV-MPC, and it shows the best performance in terms of fuel efficiency improvement. The final SOC showed a similar pattern for all the five methods.

B. VIRTUAL DRIVING SIMULATION FOCUSING ON STRAIGHT DRIVING

Scenario 2 compares and verifies the performance of the TV system on a real driving track in Fig. 13. The total distance was set to 2000 m. The Nurbuergring Grandprix Course is a track with a lot of straight-line driving, so the weight

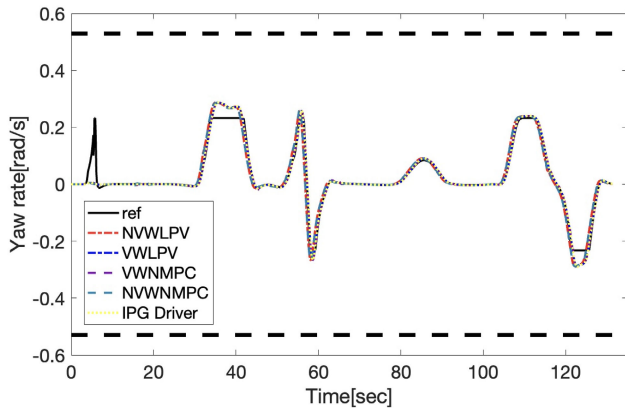


FIGURE 14. <Scenario 2> Actual vehicle yaw rate for yaw rate reference input when driving with the TV controller designed with four predictive control methods and driving of the IPG driver where the road friction coefficient and the reference vehicle speed are set as $\mu = 0.9$ and $v_{ref} = 60 \text{ km/h}$, respectively.

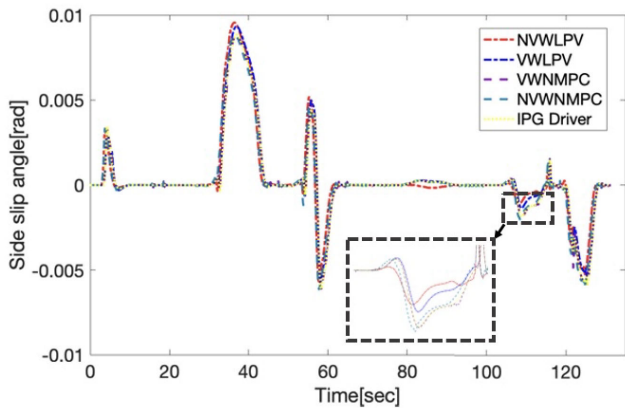


FIGURE 15. <Scenario 2> The actual vehicle side slip angle for side slip angle reference input ($\beta_{ref} = 0$) when driving with the TV controller designed with four predictive control methods and driving of the IPG driver where the road friction coefficient and the reference vehicle speed are set as $\mu = 0.9$ and $v_{ref} = 60 \text{ km/h}$, respectively.

TABLE 6. <Scenario 2> Comparison of RMSE according to yaw rate reference input when driving with the TV controller designed with four predictive control methods and driving of the IPG driver.

Control method	Reference input tracking RMSE
NVW LPV	0.0216
VW LPV	0.0216
NVW NMPC	0.0217
VW NMPC	0.0292
IPG Driver	0.0217

that considers the speed tracking (w_3) and the weight that considers the energy consumption (w_4) is increased.

In Scenario 2, the controller designed with LPV-MPC exhibited better performance in terms of yaw rate reference tracking. The reason for this is that the driving track in Scenario 2 has fewer cornering driving than in scenario 1, so the lateral acceleration, which is a condition for the single-track model to be accurate, was less than $0.4g$, and thus the

TABLE 7. <Scenario 2> Comparison of RMSE according to each reference input of side slip angle ($\beta_{ref} = 0$) when driving with the TV controller designed with four predictive control methods and driving of the IPG driver.

Control method	Reference input tracking RMSE
NVW LPV	0.0024
VW LPV	0.0024
NVW NMPC	0.0024
VW NMPC	0.0023
IPG Driver	0.0024

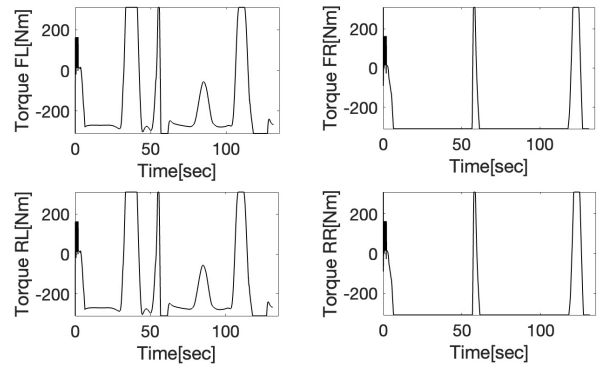


FIGURE 16. <Scenario 2> Motor demand torque applied to four in-wheel motors as a result of TV with NVW LPV-MPC applied.

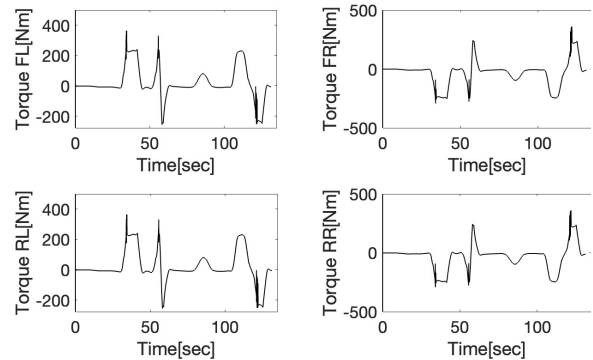


FIGURE 17. <Scenario 2> Motor demand torque applied to four in-wheel motors as a result of TV with VW LPV-MPC applied.

accuracy of the model was guaranteed. The TV system applied with NVW NMPC shows similar performance to the controller designed as a linear model, but the TV system with VW NMPC showed a higher RMSE than the other four methods. In addition, considering whether there is a change in the weight of the objective function, if the weight changes, the yaw rate RMSE increases as the weights w_1 and w_2 decrease. When comparing the RMSE as shown in TABLE 7, they are in the range of $0.0023 \sim 0.0024$, and the reference tracking performance for each side slip was similar. However, when comparing the side-slip angles in Fig. 15, LPV-MPC shows a value closer to zero than the other methods, regardless of whether weight changes.

In Scenario 2, in the case of the controller whose weight of the objective function changes, less energy is used because

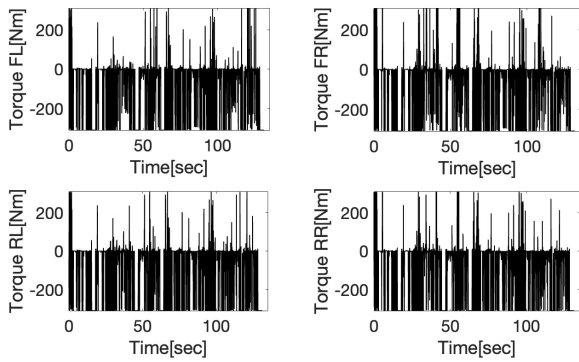


FIGURE 18. <Scenario 2> Motor demand torque applied to four in-wheel motors as a result of TV with NVW NMPC applied.

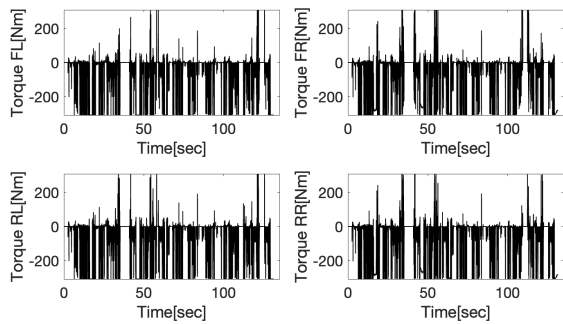


FIGURE 19. <Scenario 2> Motor demand torque applied to four in-wheel motors as a result of TV with VW NMPC applied.

TABLE 8. <Scenario 2> Comparison of energy consumption of four wheel motors when driving with the TV controller designed with four predictive control methods using motor power data of IPG CarMaker and driving with the IPG driver.

Control method	Motor energy consumption [Wh]
NVW LPV	245.7590
VW LPV	241.0510
NVW NMPC	241.6772
VW NMPC	241.0510
IPG Driver	245.4409

TABLE 9. <Scenario 2> Comparison of fuel efficiency when driving with the TV controller designed with four predictive control methods and driving with the IPG driver.

Method	Fuel efficiency [km/kWh]	Relative fuel efficiency [%]	Final SoC [-]
NVW LPV	8.2831	101.65	0.6959
VW LPV	8.3067	101.94	0.6959
NVW NMPC	8.2863	101.69	0.6959
VW NMPC	8.3067	101.94	0.6959
IPG Driver	8.1486	100	0.6959

the change in weight according to the repetition of straight driving in Scenario 2 is reflected. Table 9 shows a relatively small ascent rate of 1%, but in the case of a controller designed using the NMPC method with variable weights, the fuel efficiency increased by 1.9% as w_4 increased.

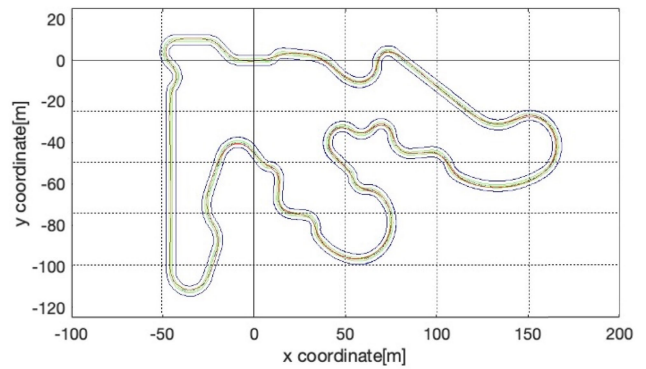


FIGURE 20. <Scenario 3> FS Germany 2006.

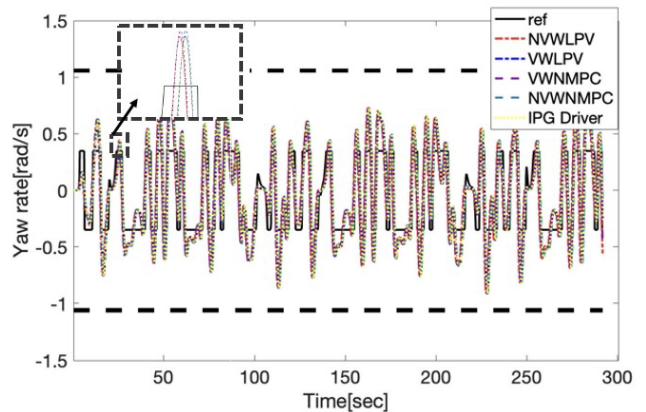


FIGURE 21. <Scenario 3> Actual vehicle yaw rate for yaw rate reference input when driving with the TV controller designed with four predictive control methods and driving of the IPG driver where the road friction coefficient and the reference vehicle speed are set as $\mu = 0.9$ and $v_{ref} = 60 \text{ km/h}$, respectively.

C. VIRTUAL DRIVING SIMULATION FOCUSING ON CORNER-DRIVING

In Scenario 3, a simulation was performed on a driving track different from that of Scenario 2 in order to observe the effect of the changing weights. The total distance was set to 2000 m. FS Germany 2006 has frequent cornering in contrast to Scenario 2, which has a lot of straight driving, and the steering angle changes frequently and has a large value in Fig. 20. In addition, more generous side slip angle constraints than Scenarios 1 and 2 were set. Therefore, w_1 and w_2 increase as the steering angle increases, which affects the tracking of the reference input of the yaw rate and side slip angle. In Fig. 21, the reference input also changed frequently according to the frequent change in the steering angle, and consequently, the change in the vehicle yaw rate is also affected.

TABLE 10 shows the lowest RMSE when the predictive control method using the nonlinear model was applied, as in Scenario 1. On the other hand, when the linear model was used, the RMSE value was higher than that of the nonlinear model. Scenario 3 is a more complex track than Scenarios 1 and 2 so that there are more frequent cornering driving situations in Scenario 3, and accordingly, the driver sometimes requests a large steering angle value. As a result, both

TABLE 10. <Scenario 3> Comparison of RMSE according to yaw rate reference input when driving with the TV controller designed with four predictive control methods and driving of the IPG driver.

Control method	Reference input tracking RMSE
NVW LPV	0.2134
VW LPV	0.1904
NVW NMPC	0.1841
VW NMPC	0.1841
IPG Driver	0.1853

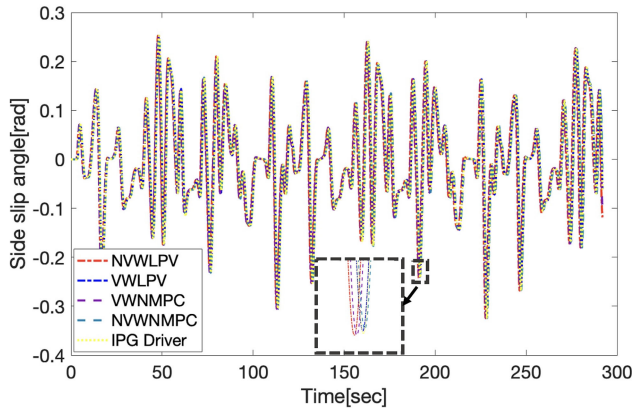


FIGURE 22. <Scenario 3> The actual vehicle side slip angle for the side slip angle reference input ($\beta_{ref} = 0$) when driving with the TV controller designed with four predictive control methods and driving of the IPG driver where $\mu = 0.9$, $v_{ref} = 60$ km/h.

TABLE 11. <Scenario 3> Comparison of RMSE according to each reference input of the side slip angle ($\beta_{ref} = 0$) when driving with the TV controller designed with four predictive control methods and driving of the IPG driver.

Control method	Reference input tracking RMSE
NVW LPV	0.0979
VW LPV	0.0979
NVW NMPC	0.0983
VW NMPC	0.0980
IPG Driver	0.0985

the RMSE for the reference input of the yaw rate and side slip angle show a lower tendency when the weight changes, as the weights w_1 and w_2 increase. In Fig. 22, unstable side slip angles occur on tracks requiring frequent cornering and large steering angle values, such as in Scenario 3. In TABLE 11, the LPV-MPC design using a linear model showed the lowest RMSE, and the IPG Driver showed the highest RMSE.

In Scenario 3, the controller whose weights did not change showed the lowest energy consumption and good performance in terms of energy efficiency, and VW NMPC showed the lowest energy efficiency. The reason for this is the change in weight, considering the motion of the vehicle. In Table 13, the controller designed with NVW LPV-MPC and NVW NMPC showed a 3.7 % improvement in fuel efficiency compared with the IPG Driver, whereas the controller designed with VW NMPC showed the lowest fuel efficiency. Thus, the weight variable controller may not show good performance in terms of energy efficiency on roads with frequent cornering

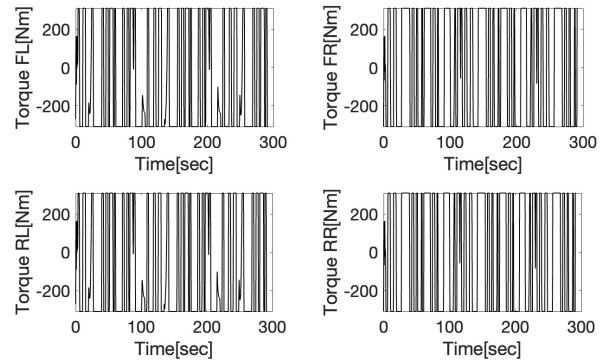


FIGURE 23. <Scenario 3> Motor demand torque applied to four in-wheel motors as a result of TV with NVW LPV-MPC applied.

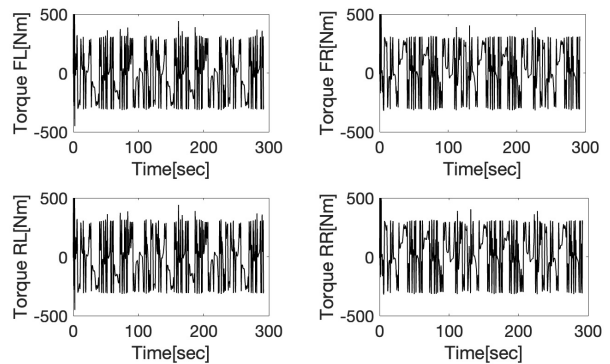


FIGURE 24. <Scenario 3> Motor demand torque applied to four in-wheel motors as a result of TV with VW LPV-MPC applied.

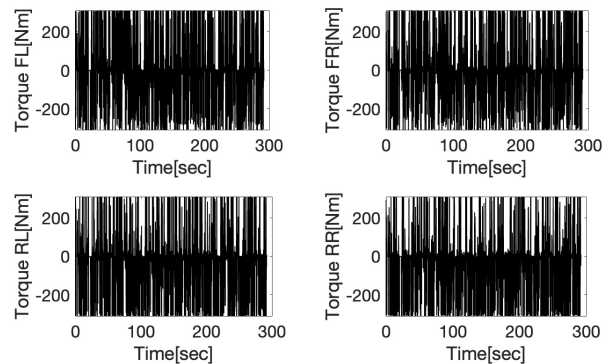


FIGURE 25. <Scenario 3> Motor demand torque applied to four in-wheel motors as a result of TV with NVW NMPC applied.

driving. As in the case of NMPC, VW LPV-MPC does not perform better than NVW LPV-MPC. The average computation time in optimization of control inputs over the prediction horizon was 0.0025 sec for LPV-MPC and 0.0035 sec for NMPC, where the computation time is calculated by measuring the time difference between calling the solver and obtaining optimal solutions in the CPU clock. Considering that the sampling-time used for simulation was 0.02 sec, the average computation time for both methods is an order of magnitude faster than sampling time-interval.

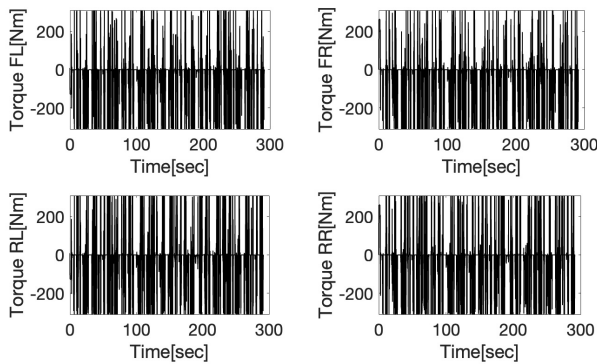


FIGURE 26. <Scenario 3> Motor demand torque applied to four in-wheel motors as a result of TV with VW NMPC applied.

TABLE 12. <Scenario 3> Comparison of energy consumption of four wheel motors when driving with the TV controller designed with four predictive control methods using motor power data of IPG CarMaker and driving with the IPG driver.

Control method	Motor energy consumption [Wh]
NVW LPV	330.0089
VW LPV	332.6871
NVW NMPC	330.0089
VW NMPC	349.6361
IPG Driver	342.2602

TABLE 13. <Scenario 3> Comparison of fuel efficiency when driving with the TV controller designed with four predictive control methods and driving with the IPG driver.

Method	Fuel efficiency [km/kWh]	Relative fuel efficiency [%]	Final SoC [-]
NVW LPV	6.0603	103.71	0.6945
VW LPV	6.0118	102.88	0.6946
NVW NMPC	6.0603	103.71	0.6945
VW NMPC	5.7202	97.89	0.6945
IPG Driver	5.8435	100	0.6945

From simulation results obtained from using Car-Maker, one might conclude that in terms of tradeoff between energy-efficiency and driving stability, the adaptive weighting predictive controller may be worse than the fixed weighting one when driving Scenarios 1 and 3 where there are frequent cornering segments. Using the adaptive weight parameter, the operating mode of the vehicle is explicitly considered so that there could be increased stability in compensation for a decrease in energy-efficiency. The weights of tracking the desired yaw rate and the side slip angle increase with larger steering angles. The weights of tracking the desired longitudinal speed and maximizing motor energy-efficiency increase with smaller steering angles. We compared and verified the performances of four different MPC controllers in three different driving scenarios. MPC with varying weights might outperform the counterparts with fixed weights in performance indices, as adaptation to dynamic driving conditions can provide more flexibility in controller design.

VI. CONCLUSION

This paper presented model predictive control methods for energy-efficient and stability-guaranteed torque vectoring for electric vehicles with four in-wheel motors. When compared with the existing IPG driver in high-fidelity Car-Maker simulations, the proposed LPV-MPC and NMPC methods achieved an energy efficiency improvement of over 2–3 % on average with similar yaw stability performance. In LPV-MPC, the reduced single-track model was applied with decoupled linearized longitudinal dynamics, whereas the full-order double-track model was applied in NMPC. In terms of computation time, LPV-MPC showed approximately 30 % faster computational speed than NMPC. In addition to the comparisons of two predictive control methods, LPV-MPC and NMPC, varying weights were applied in the cost functions to adapt to different driving conditions and requirements. Both LPV-MPC and NMPC with adaptive weights showed slightly lower energy efficiencies in cornering, whereas they showed higher energy efficiency improvements in straight driving. In NMPC, the change in the demand torque of the motor tends to be more extreme, compared to LPV-MPC. Such jerks in motor torque may cause a failure due to a large load on the motor and LPV-MPC can be more attractive in practical applications. In conclusion, it is important to design an energy-efficient TV controller with guaranteed driving stability by adopting an appropriate predictive model and weight parameters under different driving conditions and requirements. In our future work, we will implement the proposed TV systems in hardware-in-the-loop simulations to validate and verify the methods.

ACKNOWLEDGMENT

An earlier version of this paper was presented in part at the 2020 20th International Conference on Control, Automation and Systems (ICCAS) [1].

REFERENCES

- [1] S. Kim, H. Kim, J. Bae, and K.-K. K. Kim, "Linear parameter varying model predictive control for yaw-stabilizing and energy-efficient torque vectoring of in-wheel motor electric vehicles," in *Proc. 20th Int. Conf. Control, Autom. Syst.*, 2020, p. 1313.
- [2] Z. Li, A. Khajepour, and J. Song, "A comprehensive review of the key technologies for pure electric vehicles," *Energy*, vol. 182, pp. 824–839, Sep. 2019.
- [3] Y. Luo and D. Tan, "Study on the dynamics of the in-wheel motor system," *IEEE Trans. Veh. Technol.*, vol. 61, no. 8, pp. 3510–3518, Oct. 2012.
- [4] G. D. Filippis, B. Lenzo, A. Sorniotti, P. Gruber, and W. D. Nijs, "Energy-efficient torque-vectoring control of electric vehicles with multiple drivetrains," *IEEE Trans. Veh. Technol.*, vol. 67, no. 6, pp. 4702–4715, Jun. 2018.
- [5] S. Ding, L. Liu, and W. X. Zheng, "Sliding mode direct yaw-moment control design for in-wheel electric vehicles," *IEEE Trans. Ind. Electron.*, vol. 64, no. 8, pp. 6752–6762, Mar. 2017.
- [6] B. Ren, H. Chen, H. Zhao, and L. Yuan, "MPC-based yaw stability control in in-wheel-motored EV via active front steering and motor torque distribution," *Mechatronics*, vol. 38, pp. 103–114, Sep. 2016.
- [7] K. Yang, D. Dong, C. Ma, Z. Tian, Y. Chang, and G. Wang, "Stability control for electric vehicles with four in-wheel-motors based on sideslip angle," *World Electr. Vehicle J.*, vol. 12, no. 1, p. 42, Mar. 2021.
- [8] S. Koehler, A. Viehl, O. Bringmann, and W. Rosenstiel, "Energy-efficiency optimization of torque vectoring control for battery electric vehicles," *IEEE Intell. Transp. Syst. Mag.*, vol. 9, no. 3, pp. 59–74, Fall 2017.

- [9] H. Deng, Y. Zhao, S. Feng, Q. Wang, C. Zhang, and F. Lin, "Torque vectoring algorithm based on mechanical elastic electric wheels with consideration of the stability and economy," *Energy*, vol. 219, Mar. 2021, Art. no. 119643.
- [10] M. Dalboni, D. Tavernini, U. Montanaro, A. Soldati, C. Conconi, M. Dhaens, and A. Sorniotti, "Nonlinear model predictive control for integrated energy-efficient torque-vectoring and anti-roll moment distribution," *IEEE/ASME Trans. Mechatronics*, vol. 26, no. 3, pp. 1212–1224, Jun. 2021.
- [11] H. Laghmar, M. Doumiati, R. Talj, and A. Charara, "Yaw moment Lyapunov based control for in-wheel-motor-drive electric vehicle," *IFAC-PapersOnLine*, vol. 50, no. 1, pp. 13828–13833, 2017.
- [12] T. Kobayashi, E. Katsuyama, H. Sugiura, E. Ono, and M. Yamamoto, "Direct yaw moment control and power consumption of in-wheel motor vehicle in steady-state turning," *Vehicle Syst. Dyn.*, vol. 55, no. 1, pp. 104–120, Jan. 2017.
- [13] J. Park, I. Jang, and S.-H. Hwang, "Torque distribution algorithm for an independently driven electric vehicle using a fuzzy control method: Driving stability and efficiency," *Energies*, vol. 11, no. 12, p. 3479, Dec. 2018.
- [14] L. D. Novellis, "Direct yaw moment control actuated through electric drivetrains and friction brakes: Theoretical design and experimental assessment," *Mechatronics*, vol. 26, pp. 1–15, Mar. 2015.
- [15] H. Liu, L. Zhang, P. Wang, and H. Chen, "A real-time NMPC strategy for electric vehicle stability improvement combining torque vectoring with rear-wheel steering," *IEEE Trans. Transport. Electric.*, vol. 8, no. 3, pp. 3825–3835, Sep. 2022.
- [16] E. Morera-Torres, C. Ocampo-Martinez, and F. D. Bianchi, "Experimental modelling and optimal torque vectoring control for 4WD vehicles," *IEEE Trans. Veh. Technol.*, vol. 71, no. 5, pp. 4922–4932, May 2022.
- [17] P. Sun, A. S. Trigell, L. Drugge, and J. Jerrelind, "Energy-efficient direct yaw moment control for in-wheel motor electric vehicles utilising motor efficiency maps," *Energies*, vol. 13, no. 3, p. 593, Jan. 2020.
- [18] W. Xu, H. Chen, H. Zhao, and B. Ren, "Torque optimization control for electric vehicles with four in-wheel motors equipped with regenerative braking system," *Mechatronics*, vol. 57, pp. 95–108, Feb. 2019.
- [19] D. K. Perovic, "Making the impossible, possible—Overcoming the design challenges of in wheel motors," *World Electr. Vehicle J.*, vol. 5, no. 2, pp. 514–519, Jun. 2012.
- [20] M. Bicek, T. Pepelnjak, and F. Pusavec, "Production aspect of direct drive in-wheel motors," in *Proc. 52nd CIRP Conf. Manuf. Syst. (CMS)*, vol. 81, pp. 1278–1283, 2019.
- [21] C. Zhu, C. Zhao, and Z. Li, "A joint simulation for electric vehicle design based on MATLAB/simulink and CarSim," in *Proc. IEEE Int. Conf. Veh. Electron. Saf. (ICVES)*, Sep. 2019, pp. 1–6.
- [22] R. Rajamani, *Vehicle Dynamics and Control*, 2nd ed. New York, NY, USA: Springer, 2011.
- [23] H. B. Pacejka, *Tire and Vehicle Dynamics*. Oxford, U.K.: Butterworth-Heinemann, 2002.
- [24] A. Marouf, M. Djemai, C. Sentouh, and P. Pudlo, "A new control strategy of an electric-power-assisted steering system," *IEEE Trans. Veh. Technol.*, vol. 61, no. 8, pp. 3574–3589, Oct. 2012.
- [25] L. Xiong, Z. Yu, Y. Wang, C. Yang, and Y. Meng, "Vehicle dynamics control of four in-wheel motor drive electric vehicle using gain scheduling based on tyre cornering stiffness estimation," *Vehicle Syst. Dyn.*, vol. 50, no. 6, pp. 831–846, 2012.
- [26] M. Nagai, M. Shino, and F. Gao, "Study on integrated control of active front steer angle and direct yaw moment," *JSAE Rev.*, vol. 23, no. 3, pp. 309–315, 2002.
- [27] U. Kiencke and L. Nielsen, *Automotive Control Systems: For Engine, Driveline and Vehicle*, 1st ed. Berlin, Germany: Springer-Verlag, 2000.
- [28] F. Gustafsson, "Slip-based tire-road friction estimation," *Automatica*, vol. 33, no. 6, pp. 1087–1099, Jun. 1997.
- [29] M. M. Morato, J. E. Normey-Rico, and O. Sename, "Model predictive control design for linear parameter varying systems: A survey," *Annu. Rev. Control*, vol. 49, pp. 64–80, Jan. 2020.
- [30] A. Domahidi and J. Jerez. (2019). *Forces Professional*. Embotech AG, Zürich, Switzerland. Accessed: Jul. 3, 2022. [Online]. Available: <https://embotech.com/FORCES-Pro>
- [31] A. Zanelli, A. Domahidi, J. Jerez, and M. Morari, "FORCES NLP: An efficient implementation of interior-point methods for multistage nonlinear nonconvex programs," *Int. J. Control*, vol. 93, no. 1, pp. 13–29, Jan. 2020.



SANG HYUK KIM received the B.S. and M.S. degrees in electrical and computer engineering from Inha University, Incheon, South Korea, in 2020 and 2022, respectively. He is currently a Research Engineer with Hyundai Motor Company. His research interest includes embedded model predictive control for electrified vehicles.



KWANG-KI K. KIM received the M.S. and Ph.D. degrees in aerospace engineering from the University of Illinois at Urbana–Champaign, Champaign, IL, USA, in 2009 and 2013, respectively. From 2013 to 2016, he was a Postdoctoral Fellow affiliated with the School of Electrical and Computer Engineering, Georgia Institute of Technology, Atlanta, GA, USA. He was as a Senior Research Engineer with Electronics Technology Center, Hyundai Motor Company, South Korea. In 2017, he joined Inha University, where he has been an Associate Professor with the Department of Electrical Engineering, since 2023. His research interests include robotics, estimation, optimization, and control.

• • •